

II-I Molecular and Electronic Structures of Metallofullerenes

The continued interest in radical ions of fullerenes and metallofullerenes has resulted from the discovery of superconductivity in the CT complexes of alkali metals with fullerenes. Spectroscopic information concerning the electronic and spin states of the metallofullerenes has been obtained by ESR measurements.

II-I-1 A Multi-Frequency EPR Study of Endohedral Metallofullerenes Containing the Divalent Eu Ion

MATSUOKA, Hideto; FURUKAWA, Ko; KATO, Tatsuhisa; OZAWA, Norio¹; KODAMA, Takeshi¹; NISHIKAWA, Hiroyuki¹; IKEMOTO, Isao¹; KIKUCHI, Koichi¹; SATO, Kazunobu²; SHIOMI, Daisuke²; TAKUI, Takeji²
(¹Tokyo Metropolitan Univ.; ²Osaka City Univ.)

An endohedral fullerene containing a lanthanoid ion in C₈₂ cage, M@C₈₂ (M; a lanthanoid ion), has been widely investigated in the field of fullerene science. Our attention in this work has been paid to the metallofullerene containing the divalent Eu ion with the highest spin ($S = 7/2$) of lanthanoid ion, focusing on the surrounding symmetry of the ion. We isolated three isomers of Eu@C₈₂ with the cage structures of C_s, C₂, and C_{2v} symmetry, and Eu@C₇₄ with that of D_{3h} symmetry. Their formal electronic structures are represented by Eu²⁺@C_n²⁻ ($n = 74$ or 82), where two electrons of Eu atom transfer to the cages. In this work, multi-frequency Electron Paramagnetic Resonance (EPR) measurements were performed to determine their spin-Hamiltonian parameters related to the surrounding symmetry of Eu²⁺ ion. Figure (a) shows W-band EPR spectrum observed for Eu@C₇₄ at 4 K. The spin-Hamiltonian parameters were precisely determined by spectral analysis including higher-order zero-field splitting (ZFS) terms. Figures (b) and (c) show the W-band CW-EPR spectra calculated for Eu@C₇₄ by using positive and negative D values, respectively. Figure (b) was in good agreement with the observed spectrum, concluding that Eu@C₇₄ has the positive D value. A non-zero rhombicity parameter E/D ($= 0.11$) was obtained for Eu@C₇₄, indicating that Eu(II) ion is not at the center of the C₇₄ cage. The spin-Hamiltonian parameters including the signs of the D values for the other sample were also determined in this manner.

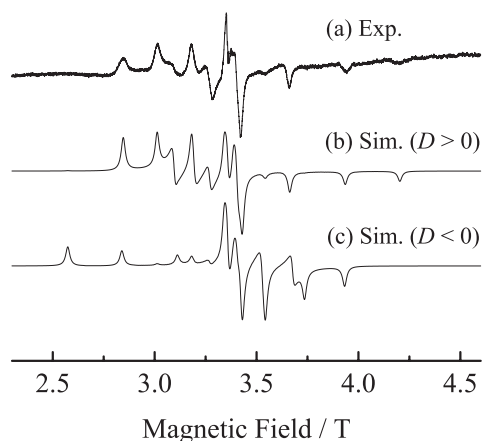


Figure 1. W-band EPR spectra of Eu@C₇₄: (a) experiment; (b) simulation ($D > 0$); and (c) simulation ($D < 0$). Experimental conditions: microwave frequency, 95 GHz; temperature, 4 K.

II-I-2 Study on the Electron Spin State of La₂@C₈₀ Anion

KATO, Tatsuhisa; MATSUOKA, Hideto; OKUBO, Shingo¹; DINSE, Klaus-Peter²
(¹RIKEN; ²Darmstadt Tech. Univ.)

An anion form of a lanthanum dimer with C₈₀ cage (La₂@C₈₀⁻) was obtained by chemical and electrochemical reduction. The La₂@C₈₀⁻ anion exhibited the characteristic Electron Spin Resonance (ESR) pattern for the spin-doublet radical having very large hyper fine coupling (hfc) interaction with the identical two La nuclei, as seen in Figure. The exact values of hfc and g-tensor were determined by ESR measurements with two different frequencies, *i.e.* 9.5 GHz (X-band) and 95 GHz (W-band). The spectrum was completely simulated by parameters shown in Figure. Two La ions were identical, however, they formed a dimer and were fixed at the certain position within the C₈₀(I_h) cage. The total symmetry of La₂@C₈₀⁻ anion was D_{2h}. The picture of the electronic state was changed from those of a neutral form of La₂@C₈₀ by the injection of an excess electron.

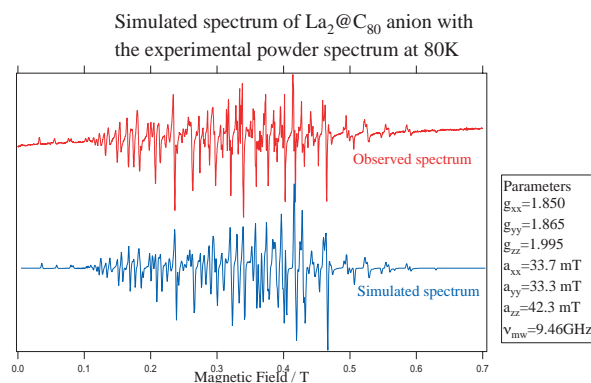


Figure 1. The ESR spectrum of La₂@C₈₀⁻ anion. The upper spectrum was obtained by a 9.5 GHz (X-band) spectrometer, the lower one was obtained by the simulation using the parameters indicated in the right box.

II-I-3 Spin States of Water-Soluble C₆₀ and Metallofullerenes

KATO, Tatsuhisa; MATSUOKA, Hideto; FURUKAWA, Ko; KATO, Haruhito¹; SHINOHARA, Hisanori¹; HUSEBO, Lars Olav²; WILSON, Lon J.²
(¹Nagoya Univ.; ²Rice Univ.)

Nagoya group of author has shown an application of water-soluble metallofullerenes to magnetic resonance imaging (MRI) contrast agents.¹⁾ It has been found *in vivo* and *in vitro* that water-soluble polyhydroxylated gadolinium metallofullerenols,²⁾ $\text{Gd@C}_{82}(\text{OH})_n$, exhibit a very strong ability of reducing water proton relaxation times, T_1 and T_2 , which results a high MR signal enhancement. This property would be originated from the magnetization due to $4f^7$ radical electrons of Gd^{3+} ion. However, spin states of polyhydroxylated fullerenols have not been clarified in detail. We investigated spin states of $\text{C}_{60}(\text{OH})_n$, $\text{La@C}_{82}(\text{OH})_n$, $\text{La}_2\text{-C}_{80}(\text{OH})_n$, and $\text{Gd@C}_{82}(\text{OH})_n$ in aqueous solution by using cw-electron spin resonance (cw-ESR) and pulsed-ESR spectrometers. $\text{Gd@C}_{82}(\text{OH})_n$ gave a broad cw-EPR spectrum which was characterized by the high spin state of $S = 7/2$, as shown in Figure 1. The other samples in frozen solution showed cw-ESR signal around $g = 4$ as well as $g = 2$. These spectra could be attributed to the spin state of higher spin than $S = 1/2$. Actually the nutation frequency corresponding not only to $S = 1/2$ but also to $S = 1$ was observed by 2D- nutation measurements. $\text{C}_{60}(\text{OH})_n$, $\text{La@C}_{82}(\text{OH})_n$, and $\text{La}_2\text{-C}_{80}(\text{OH})_n$ exhibit ESR spectra due to the spin state of $S = 1$, and its magnetization gives the ability of reducing water proton relaxation times in MRI measurement.

References

- 1) M. Mikawa *et al.*, *Bioconjugate Chem.* **12**, 510–514 (2001).
- 2) H. Kato *et al.*, *Chem. Phys. Lett.* **324**, 255–259 (2000).

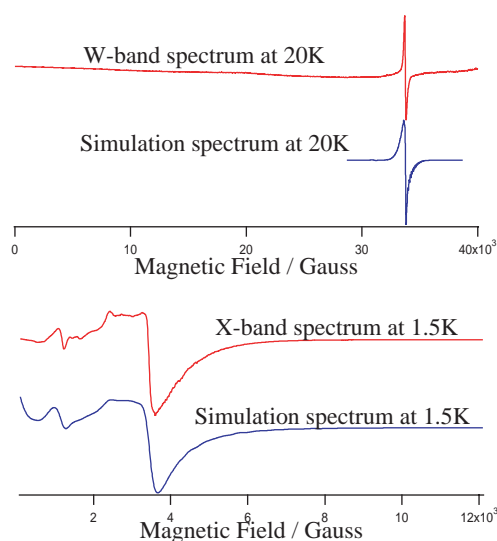


Figure 1. EPR spectra of $\text{Gd@C}_{82}(\text{OH})_n$ obtained by a 9.5 GHz (X-band) spectrometer, the lower trace, and by a 95 GHz (W-band) one, the upper trace.

II-I-4 Chemical Reactivity and Redox Property of $\text{Sc}_3\text{@C}_{82}$

KATO, Tatsuhisa; KOBAYASHI, Kaoru; NAGASE, Shigeru; WAKAHARA, Takatsugu¹; IIDUKA, Yuko¹; SAKURABA, Akihiro²; OKAMURA, Mutsuo²; TSUCHIYA, Takahiro¹; MAEDA, Yutaka¹; ISHIZUKA, Midori O.¹; AKASAKA, Takeshi¹; KADISH, Karl M.³

(¹Univ. Tukuba; ²Niigata Univ.; ³Univ. Houston)

The photochemical and thermal reactions of $\text{Sc}_3\text{@C}_{82}$ with disilrane afforded an exohedral adduct indicating the high reactivity of $\text{Sc}_3\text{@C}_{82}$. The redox potentials of $\text{Sc}_3\text{@C}_{82}$ in *o*-dichlorobenzene show a high electron affinity and a small band gap. The $\text{Sc}_3\text{@C}_{82}$ anion was prepared by electrochemical reduction, which possesses a diamagnetic character. Recently, we have accomplished the chemical reduction of endohedral metallofullerenes as La@C_{82} and $\text{La}_2\text{@C}_{80}$ in the pyridine and DMF solution. In this context, $\text{Sc}_3\text{@C}_{82}$ may exist as an anionic form in pyridine. No ESR signal was observed at room temperature in the ESR spectrum of $\text{Sc}_3\text{@C}_{82}$ in the presence of pyridine, indicating the formation of the diamagnetic $\text{Sc}_3\text{@C}_{82}$ anion (Figure 1). After removal of pyridine, the residue was resolved again in toluene. Interestingly, the ESR spectrum of $\text{Sc}_3\text{@C}_{82}$ was recovered, and it was accompanied by a triplet spectrum at $g = 2.0403$, as can be seen in Figure 1. The recovered spectrum was identical with the original $\text{Sc}_3\text{@C}_{82}$ one in terms of g -value, 1.9985, and isotropic hfs constant, 6.25 gauss. The accompanying triplet splitting would come from the hfs of ^{14}N nucleus, which would be due to a by-product of chemical reduction by pyridine. These observations surely reveal that $\text{Sc}_3\text{@C}_{82}$ can exist as an anionic form in pyridine.

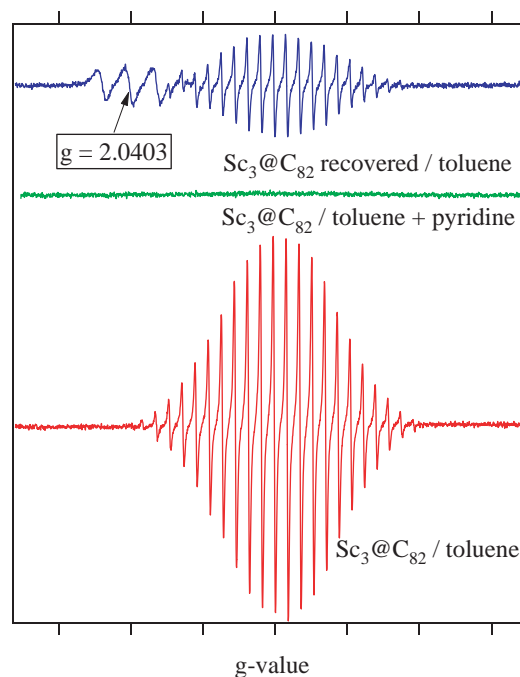


Figure 1. Twenty two lines of ESR spectrum of $\text{Sc}_3\text{@C}_{82}$ in toluene, the lower trace, disappeared in the presence of pyridine as shown in the middle trace, indicating the formation of the diamagnetic $\text{Sc}_3\text{@C}_{82}$ anion. After removal of pyridine, the residue was resolved again in toluene and exhibited the ESR spectrum of $\text{Sc}_3\text{@C}_{82}$. It was accompanied by a triplet spectrum at $g = 2.0403$. The recovered spectrum was identical with the original $\text{Sc}_3\text{@C}_{82}$ one in terms of g -value, 1.9985, and isotropic hfs constant, 6.25 gauss.

II-I-5 Hyperfine Interactions in La@C₈₂ Studied by W-Band EPR and ENDOR

KATO, Tatsuhisa; WEIDEN, Norbert¹; DINSE, Klaus-Peter¹

(¹Darmstadt Tech. Univ.)

The analysis of dipolar and quadrupolar lanthanum hyperfine data measured with EPR and ENDOR reveals that at low temperatures no significant change occurs at the internal binding site of the endohedral complex. We interpret this result as indicative of freezing of the large-scale motion of the encased ion, which is observed at room temperature. Averaging of hyperfine interactions is fast on the time scale of the EPR experiment, preventing drastic changes of dipolar and quadrupolar hfi, providing that the equilibrium position is unchanged. The detection of hyperfine interaction in disordered samples was possible by invoking orientation selection in the 94 GHz EPR spectrum. Quadrupolar hfi could be directly measured for the first time in a metallo-endohedral fullerene complex.

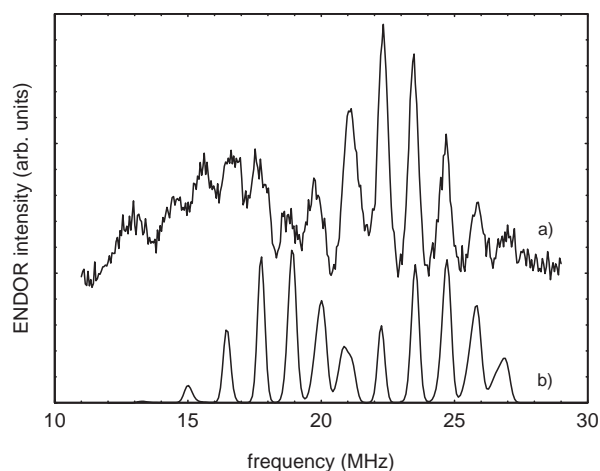


Figure 1. a) W-band pulsed ENDOR spectrum of La@C₈₂(I) measured at 10 K at $B_0 = 3371.6$ mT. The spectrum was accumulated when exciting the high-field edge of the EPR spectrum and by invoking a Davies pulse sequence. b) A simulated spectrum used to identify the individual line positions is also shown.

II-J High Field and Pulsed Electron Spin Resonance Spectroscopy

Electron paramagnetic resonance (EPR) spectroscopy has been a powerful technique for the characterization of radical species. The modern development of EPR spectroscopy enables us to investigate the heterogeneous and disordered system in detail. Especially the high frequency and pulsed EPR methods achieve the substantial resolution enhancement of spectrum. The advanced EPR spectroscopy is applied to study on the spin state in the heterogeneous system.

II-J-1 A Discrete Self-Assembled Metal Array in Artificial DNA

KATO, Tatsuhisa; TOYAMA, Namiki; TANAKA, Kentaro¹; TENGEIJI, Atsushi¹; SHIONOYA, Mitsuhiro¹

(¹Univ. Tokyo)

[*Science* **299**, 1212–1213 (2003)]

DNA has a structural basis to array functionalized building blocks. Here we report the synthesis of a series of artificial oligonucleotides, d(5'-GH_nC-3') ($n = 1$ to 5), with hydroxypyridone nucleobases (H) as flat bidentate ligands. Righthanded double helices of the oligonucleotides, $n\text{Cu}^{2+}$ d(5'-GH_nC-3')₂ ($n = 1$ to 5), were quantitatively formed through copper ion (Cu²⁺) -mediated alternative base pairing (H-Cu²⁺-H), where the Cu²⁺ ions incorporated into each complex were aligned along the helix axes inside the duplexes with the Cu²⁺-Cu²⁺ distance of 3.7 ± 0.1 angstroms. The Cu²⁺ ions were coupled ferromagnetically with one another through unpaired *d* electrons to form magnetic chains. Continuous-wave electron paramagnetic resonance (CW-EPR) spectra of the duplexes Cu-*n* ($n = 1-5$) in a

frozen aqueous solution were recorded at 1.5 K by a conventional X-band spectrometer (Figure 1). The spectrum of the mononuclear complex Cu-1 was reproducible in a simulation as arising from a doublet ($S = 1/2$) radical of a Cu²⁺ center in the square-planar ligand field. However, spectra of Cu-2, Cu-3, Cu-4, and Cu-5 exhibited quite different patterns from that of Cu-1. The spectrum of Cu-2 could be attributed to the spin state of $S = 1$, that of Cu-3 to $S = 3/2$, and those of Cu-4 and Cu-5 to $S = 2$ and $S = 5/2$, respectively. The results obtained by CW-ESR spectra were confirmed by the Transient Nutation measurement of a pulsed-ESR. With accumulating Cu²⁺ ions, the electron spins on adjacent Cu²⁺ centers are aligned parallel and couple in a ferromagnetic manner, with Cu-*n* ($n = 1-5$) attaining the highest spin state, as expected from a lineup of n Cu²⁺ ions.

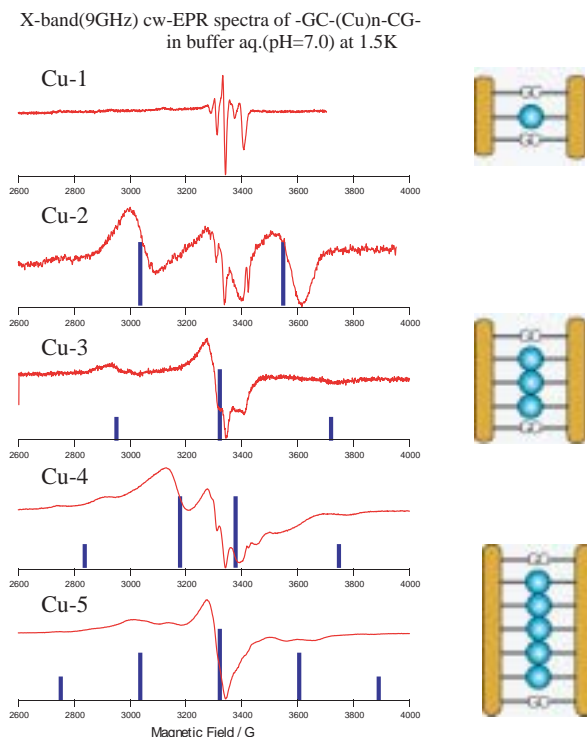


Figure 1. CW-EPR spectra of the duplexes Cu- n ($n = 1-5$) in frozen aqueous solution at 1.5 K, recorded by an X-band spectrometer with a 9.5-GHz microwave.

II-J-2 Charge Transport in the Insulating State of (DMe-DCNQI) $_2$ Li above T_{SP} : A Possible Fractional Charge Soliton Conduction with $\pm \frac{1}{2}e$

KATO, Tatsuhisa; HIRAOKA, Maki¹;
SAKAMOTO, Hirokazu¹; MIZOKUCHI, Kenji¹;
KATO, Reizo²
(¹Tokyo Metropolitan Univ., ²RIKEN)

[Phys. Rev. Lett. **91**, 056604 (2003)]

A spin-Peierls system (DMe-DCNQI) $_2$ Li is studied with W-band electron paramagnetic resonance (EPR) (94 GHz) to unveil a charge transport mechanism in the insulating $4k_F$ charge density wave state above T_{SP} . The electron hopping between the neighbor DCNQI columns provides an additional broadening of the EPR linewidth, since the neighbor columns are generally nonequivalent to each other with respect to g shift. The obtained intercolumn hopping rates lead us to the conclusion that the electron hopping to a hole soliton carrying a fractional charge of $e/2$ in the neighbor column dominates the intercolumn charge transport.

II-J-3 Magnetic Properties for Hexaphyrin

FURUKAWA, Ko; KATO, Tatsuhisa;
VENKATARAMANARAO, G. Arnan¹; SHIMIZU,
Soji¹; ARATANI, Naoki¹; OSUKA, Atsuhiko¹
(¹Kyoto Univ.)

Magnetic properties for the hexaphyrin **1** with the Cl

and O bridging ligands, the hexaphyrin **2** without the bridging ligand, and the hexaphyrin **3** with the O bridging ligand (see Figure 1) were examined. In these hexaphyrins **1-3**, not the direct exchange coupling between the Cu ions but the superexchange coupling *via* the bridging ligands is expected due to the much long Cu-Cu distance. These systems are the attractive materials from the viewpoint of the superexchange interaction.

Figure 1 shows the temperature dependence of the $\chi_p T$ values for **1-3**. The observed values were reproduced by the typical spin hamiltonian $H = -2JS_i \cdot S_j$, where J denotes the exchange coupling parameters ($J/k_B = -17.3$ K for **1**, $J/k_B = -230$ K for **3**). The $\chi_p T$ values for **2** are independent of the temperature. The spin structures for both hexaphyrins **1** and **3** have the singlet ground states. The remarkable points are the following two; (1) the exchange coupling for both **1** and **3** is antiferromagnetic, although the superexchange interaction should be ferromagnetic according to the Goodenough-Kanamori-Anderson (GKA) rule¹) and (2) the J/k_B value for **3** is much larger than that for **1**.

The GKA rule is assumed that the d orbital for the metal ions and the degenerated p orbitals for the bridging ligand take part in the superexchange interaction. The antiferromagnetic superexchange interaction is induced by the breakdown of the degeneracy of the p orbitals, which is caused by the chemical bond between the ligand O and the C atom on the hexaphyrin ring. In the hexaphyrin **1**, the superexchange interaction for the Cu-Cl-Cu pathway becomes ferromagnetic because of the equivalency between the p orbitals of the ligand Cl. Totally, the exchange coupling in **1** is weaker than that for **3**.

Reference

1) J. Goodenough, *Magnetism and the Chemical Bond*, John Wiley and Sons; New York (1963).

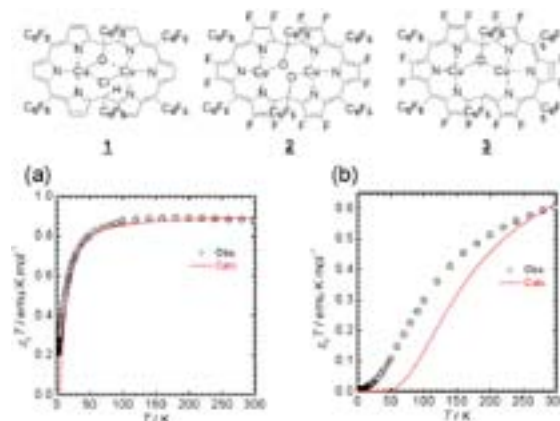


Figure 1. Temperature dependence of the $\chi_p T$ values for hexaphyrin (a) **1**, (b) **3**. The circles and lines stand for the observed and calculated values.

II-J-4 Determination of Spin State and Observation of ESEEM for Di- and Tri-Cation of Oligoanilines

KATO, Tatsuhisa; HIRAO, Yasukazu¹; ITO,
Akihiro¹; TANAKA, Kazuyoshi¹

(¹Kyoto Univ.)

The ESR spectroscopy showed that high-spin species were generated by chemical oxidation of N,N,N',N',N'',N'''-Hexakis[4-(di-4-anisylamino)-phenyl]-1,3,5- benzenetriamine in solution. The polycationic species formed by two equivalent of oxidant was assigned to be the triplet spin state, and that by three equivalent of oxidant to be the quartet spin state, respectively, on the basis of ESR spectroscopy. The assignment was confirmed by the 2 dimensional nutation (2D Nutation) measurement of pulsed ESR spectroscopy. Each polycation exhibited the specific ESEEM (Electron Spin Echo Envelope Modulation) frequency in 2-pulsed and 3-pulsed echo-decay measurement. And they gave the auto-correlation peak at the frequency associated with ESEEM in the two dimensional spectrum obtained by the HYSORE (hyperfine sublevel correlation spectroscopy) sequence.

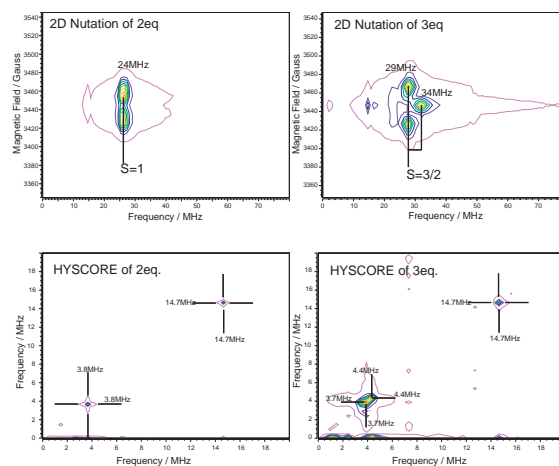


Figure 1 The upper two contour maps are 2D Nutation spectra for the di-cation and the tri-cation. The lower two contour maps are HYSORE spectra for the di-cation and the tri-cation.

II-K State Correlated Raman Spectroscopy

The vibrational Raman polarizability tensor responds to molecular reorientational relaxation process, and the structural environment in condensed media. The measurement of Raman scattering is a powerful technique for the investigations of molecular structure, molecular motion, and the mechanism of phase transition. We've built up the system of multichannel type detection of Raman scattering combined with the temperature controlled cell.

II-K-1 Intrinsic Aspect of V-Shaped Switching in Ferroelectric Liquid Crystals: Biaxial Anchoring Arising from Peculiar Short Axis Biasing in the Molecular Rotation around the Long Axis

HAYASHI, Naoki; KATO, Tatsuhisa; ANDO, Tomohiro¹; FUKUDA, Atsuo²; KAWADA, Sachiko³; KONDOH, Shinya³
(¹Shinshu Univ.; ²Univ. Dublin; ³Citizen Watch Co., Ltd.)

[*Phys. Rev. E* **68**, 11702 (2003)]

To clarify the intrinsic aspect of practically usable thresholdless V-shaped switching in ferroelectric liquid crystals, we have observed textures and measured polarized Raman scattering as well as optical transmittance in a thin homogeneous cell of a single compound by applying an electric field. The results indicate that the so-called surface stabilized ferroelectric states are destabilized, and that there exist rather stable two domains [Figure 1(a)] with broad and narrow molecular orientational distributions, both of which show the almost ideal V-shaped switching with considerably low transmittance at the tip of the V [Figure 1(b)]. We have concluded that the main cause of the V-shaped switching is the biaxial anchoring on the substrates coated with polyimide, which makes the most polarizable short axis normal to the substrates. It is in a competition with the ordinary anchoring that favors the

director parallel to the substrates, when the material has such a bulk intrinsic property that this short axis is parallel to the tilt plane. The competition makes the total anchoring energy almost independent of the azimuthal angle and gives rise to the V-shaped switching.

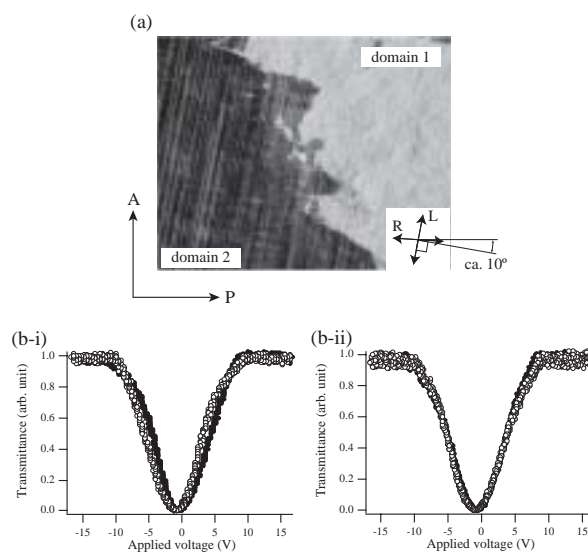


Figure 1. (a) Optical micrographs of textures taken after the long-term switching. The arrow "L" indicates the layer direction and the arrow "R" indicates the rubbing direction.

(b) Electro-optic responses observed in domains 1 [(b-i)] and 2 [(b-ii)]. Solid and open circles were obtained by increasing and decreasing the applied electric field, respectively.

II-K-2 A Large Tilt in the Core Relative to the Molecular Rotational Long Axis as Observed by Polarized Raman Scattering in a de Vries Smectic-A Liquid Crystal

HAYASHI, Naoki; KATO, Tatsuhisa; FUKUDA, Atsuo¹; PANARIN, Yuri P.¹; VIJ, Jagdish K.¹; NACRI, J.²; SHASHIDHAR, R.²; KAWADA, Sachiko³; KONDOH, Shinya³
 (¹Univ. Dublin; ²Naval Research Laborator; ³Citizen Watch Co., Ltd.)

The second- and fourth-order orientational order parameters of the core part of the molecule, $\langle P_2 \rangle$ and $\langle P_4 \rangle$, have been measured by polarized vibrational Raman spectroscopy for a homogeneously aligned ferroelectric smectic liquid crystal with three dimethyl siloxane groups in the achiral alkyl terminal chain, which shows the de Vries-type phenomena; very large electroclinic effect in the smectic-A (Sm-A) phase and a negligible layer contraction at the phase transition between the Sm-A and Sm-C* phases. The orientational order parameters of the rigid core part of the molecule are extremely small both with and without the external electric field in Sm-A; $\langle P_4 \rangle$ is only approximately 0.1 while the apparent tilt angle reaches at 32° when a sufficiently high electric field is applied to the cell. This result indicates that the core part is tilted by $26\text{--}36^\circ$ relative to the molecular rotational long axis (Figure 1).

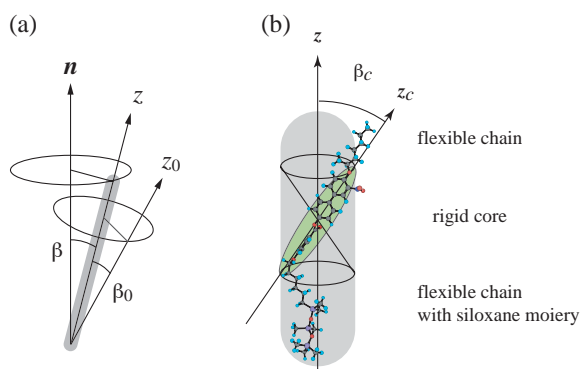


Figure 1. Schematic illustrations representing (a) the molecular rotational long axis (the z axis), the averaged direction of the molecular rotational long axes (the in-layer director, \mathbf{n}), and the longest principal axis of the Raman tensor (the z_0 axis), and (b) the molecular rotational long axis (the z axis) and the long axis of the core part (the z_c axis). Here β is the molecular tilt angle at an instant of time, β_0 the angle between the z and z_0 axes, and β_c the angle between the z and z_c axes. The molecules are rotating freely around their long axes, of which the distribution around the in-layer director is uniaxial. The z_c and z_0 axes are almost parallel each other and hence we assume $\beta_0 = \beta_c$. The conformation of the chemical structure illustrated is not a real one but is drawn just for the ease of understanding.